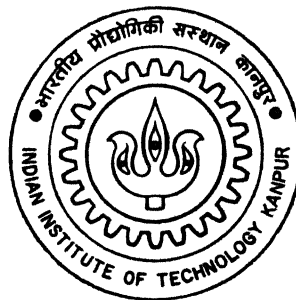# KINETICS OF CEMENTITE COARSENING IN QUENCHED AND TEMPERED EUTECTOID STEEL

by

MANAS KANTI GHOSH

Department of Materials and Metallurgical Engineering

INDIAN INSTITUTE OF TECHNOLOGY KANPUR

APRIL, 1996

KINETICS OF CEMENTITE COARSENING IN QUENCHED AND TEMPERED EUTECTOID STEEL

A Thesis Submitted

in Partial Fulfilment of the Requirements

for the Degree of

MASTER OF TECHNOLOGY

by

MANAS KANTI GHOSH

to the

DEPARTMENT OF MATERIALS AND METALLURGICAL ENGINEERING

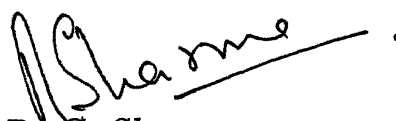## INDIAN INSTITUTE OF TECHNOLOGY KANPUR

APRIL 1996

**Dedicated
to
my friends**

CERTIFICATE

This is to certify that the present work, entitled **"Kinetics of Cementite Coarsening in Quenched and Tempered Eutectoid Steel"** by Mr. Manas Kanti Ghosh has been carried out under my supervision and to my knowledge it has not been submitted elsewhere for a degree.

Dr. R. C. Sharma.

(Professor)

Department of Materials and Metallurgical

Engineering.

Indian Institute of Technology.

Kanpur - 208016. India.

Date ·- 22th April. 1996

ACKNOWLEDGEMENT

SYNOPSIS

In the present study coarsening kinetics of cementite in quenched and tempered eutectoid steel was investigated. The steel samples were austenitised at 850°C for an hour followed by water quenching Then they were tempered at five different temperatures (625, 650, 675, 700 and 725°C) for 2 to 96 hours

Particle size distribution and average particle size were measured from the micrographs taken in scanning electron microscope using secondary electron mode at various magnifications ranging from ×1000 to ×7000 From the coarsening data, it is concluded that the coarsening takes place by carbon volume diffusion control according to Lifshitz-Slyozov-Wagner theory. The activation energy for the cementite coarsening obtained from the rate constants at different temperatures. The activation energy was found to be 82.65 kJ/mol. This value compares well with the experimental values for cementite coarsening in plain carbon steels as well as with the activation energy for carbon volume diffusion in ferrite available in literature The particle size distribution attend a pseudo steady state as expected from LSW theory.

Contents

List of Tables

i

List of Figures

Chapter 1

Inroduction

Among the metals and its various alloys steel is finding a wide range of application starting from aerospace, automotive industries to day to day domestic applications. The eutectiod steel, a particular class of "steels" as a whole, has a number of potential applications e.g. locotyres, rail tracks, ropes, cutting tools, forging dies etc [1]. The presence of tiny, hard particles in a relatively soft matrix of the steel is of primary interest in research because the size and size distribution of all these particles influence the mechanical properties of the steel to a great extent.

To get optimum properties of the material we have to have suitable microstructure. Properties such as fracture toughness, fatigue strength etc. are dependent on the particle morphology. Optimum toughness alongwith good strength can be obtained with finer particles. Smaller particles offer a well bounded interface by which microvoid formation can be avoided. Particle should be in the range of 100 $\overset{\circ}{A}$ or less for a good combination of mechanical properties. Small particles minimise the oppertunity for multiple slip band pile ups, which would greatly increase the local pile up stress and create decohesion or particle fracture [2]. Small particles should be as widely spaced as possible to avoid the overlap of stress fields. This imposes a volume fraction limit of about 10%. Particles should be spherical to avoid stress concentration associated with sharp corners. Equiaxed particles help into avoiding the multiple pile up effects. For coherent or semicoherent particles, where dislocations by pass the particles instead of cutting them, are preferred to have better toughness. An austempered steel is found to work better than a quenched and tempered steel from the fatigue property point of view [3]. The reason is that due to tempering of the steel, a thin carbide film is produced which results in a stress concentration effect. For the quenched and tempered steels the fatigue limit increases with decreasing tempering temperature [4].

1

Now to get a particular microstructure, specific heat treatment should be done and during this heat treatment solid to solid phase transformation occurs. Some of the transformation require transport of atoms over long distances rather than just across an interface. Such transformations include the precipitation reaction, the eutectiod transformations and the celluler transformations. During the later stages of diffusional transformations, the system reduces its free energy by decreasing the area of the interphase interface while the volume fractions of the phases change only slightly. This process is known as coarsening. Coarsening generally involves long range transport of atoms. In many tranformations nucleation and growth are followed by coarsening. The study of coarsening kinetics helps us in understanding the nature of transformation in a better way.

Chapter 2

Literature Review

2.1 Introduction

The microstructure of a two-phase alloy is always unstable if the total interfacial energy is not a minimum. Therefore, a high density of small precipitates will tend to coarsen into a lower density of larger particles with a smaller total interfacial area. However, such coarsening often produces an undesirable degradation of properties such as a loss of strength or the disappearance of grain-boundary pinning effects [5]. As with the grain growth, the rate of coarsening increases with temperature and is of particular concern in the design of materials for high temperature applications.

2.2 Particle Coarsening

Where dispersed particles have some solubility in the matrix in which they are contained, there is a tendency for the smaller particles to dissolve and for the material in them to precipitate on larger particles. The driving force is derived from the consequent reduction in total interfacial energy and ultimately only a single large particle would exist. The problem of deriving a function that describes the rate of change of size of any particle must take into account the relationship between particle solubility and size, the rate-controlling step of material transfer, whether movement across the particle/matrix interface or diffusion through the matrix is involved, and the particle size distribution in the system.

2.2.1 Mechanisms of Particle Coarsening

There are number of coarsening mechanisms. These are

a) Volume diffusion-controlled,

b) Grain boundary diffusion-controlled,

c) Ledge mechanism,

d) Interface controlled.

e) Diffusion through dislocations,

When the rate controlling mechanism is the diffusion of solute through the regular lattice sites, the coarsening mechanism is said to be volume diffusion controlled (VDC) In order to establish a function relationship between the particle size and the time of coarsening, it is essential to make some simplified assumptions. These are

1) The concentration gradient is considered to be time independent. This will allow us to use the Fick's First law to adequately describe the concentration gradient under steady state conditions.

2) The solute diffusion coefficient is independent of concentration of the solute. This condition will again be fulfilled because dilute solutions are generally used in precipitation studies.

3) The interfacial energy of the matrix/precipitate is independent of the radius of curvature. This is quite true of large particles. However, when precipitate particles get to a size below 100 $\overset{\circ}{A}$ or so, the value of the interfacial energy becomes critical. Since the size of the particle at the termination of growth is of the order of 100 $\overset{\circ}{A}$, the interfacial energy will not be seriously affected during coarsening. Thus a constant value of the interfacial energy will be assumed for the entire coarsening process.

4) For spherical particles, the effective diffusion distance is considered to be proportional to the radius of curvature of the particle. The value of the proportionality constant, which in reality is a complicated non-analytical function of several variables, is assumed to remain constant during the entire coarsening process.

Volume Diffusion Controlled Coarsening

This mechanism of particle coarsening was first proposed by Lifshitz and Slyozov [6] and then modified by Wagner [7]. This mechanism sometimes termed as LSW theory. This theory of particle coarsening is applicable only when the volume fraction of the precipitate is very small. Under this condition, the mean distance between particles is large compared to the dimension of the particle. Since the kinetics of coarsening is controlled by the diffusion of solute atom from a particle which is dissolving to a particle which is growing, it is expected that the mean distance between particles which is controlled in tern by the volume fraction of the precipitate will influence the rate of growth. As the volume fraction of the precipitate increases, the mean

4

separation between particles decreases and the distance that solute atoms have to diffuse on an average to become a part of the growing precipitate becomes shorter.

Coarsening of Grain Boundary Allotriomorphs

Grain boundaries may play an important role in particle growth, since the particles may nucleate preferentially on grain boundaries. For particles situated at grain boundaries the transfer of solute atoms from smaller to larger particles can occur through the boundary. This will be especially so at low temperatures where the rate of volume diffusion is lower.

The boundary controlled coarsening of precipitates situated at grain boundaries has been treated by a number of investigators. Slyozov et. al. [8] were the first investigators to show that the average size of the particles at the grain boundaries increased one-forth power of time. An independent derivation was made by Speight [9] confirming the results of Slyozov et. al.. Following Wagners method of volume diffusion controlled coarsening, Kirchner [10] used the equation derived by Speight and derived an expression for the steady state particle size distribution.

In all the above cases, it is assumed that the volume fraction of the precipitate phase in the alloy is very small and remains constant during coarsening. In the theoretical treatment of the coarsening of the grain boundary precipitate it is assumed that the diffusion of solute is confined to the plane of grain boundary. The diffusion geometry for an individual particle is cylindrical concentric with the centre of projection of the particle in the grain boundary plane. As with the volume diffusion controlled coarsening the diffusion of solute is considered to occur under steady state conditions.

Coarsening by the Ledge Mechanism

Formation of coherent interface between the precipitate and matrix phases is a common occurance. Such interfaces generally maintain a rigid habit and orientation relationship with the matrix. Widmanstatten ferrite plates having Kurdjumov-Sachs [11] orientation relationship with the parent austenite is one such example. Coherent interface of very low energy are also observed with the γ' precipitate/matrix interfaces in Ni base alloys with Si, Al and Ti [12-14]. The mobility of interfaces is critically dependent upon the structure of interfaces and their misorientation. Since, coherent interfaces have high degree of coincidence between lattices on the two sides of the interface they will have relatively low mobility. Thus the rate of growth of such ordered

boundaries is very low. The rate of growth can be enhanced if coherent interfaces have disordered steps (ledge) few atomic spacing high. The total interfacial energy will not get affected but with a highly mobile disordered interface rapid diffusion of solute can be realized. Thus coarsening can occur by the migration of ledges which act as a conduit for solute diffusion from the matrix to the growing precipitate particles.

Interface Controlled Coarsening

There is still another basic possibility under which particle growth can occur. In this case, the precipitate is assumed to differ in composition from the matrix. However, here the growth rate is controlled by the mechanism that allows the solute atoms to cross over from the matrix to the precipitate Thus, suppose that the time required for it to diffuse to the interface. In this case the solute concentration in the matrix will remain effectively constant throughout the matrix [15]. However, with continued growth of the precipitate, the level of the concentration in the matrix has to fall. This means that the driving force for growth also has to fall, since it is directly related to the degree of supersaturation.

2.2.2 Particle Size, Shape and Solubility

The simplest relationship of particle size and solubility is for a spherical particle of radius r, non-coherent with the matrix, where the interfacial energy γ is independent of orientation. This relationship is often termed as the Gibbs-Thomson or Thomson-Freundlich equation and is written

$$ln\left(\frac{S_r}{S}\right) = \frac{2\gamma\Omega}{kTr} \tag{2.1}$$

where S is the solubility of a particle of infinite radius, S_r is the solubility of a particle of radius r containing atoms of atomic volume Ω , k is Boltzmann's constant, and T is the absolute temperature [16]. Since in practice, $2\gamma\Omega \ll kTr$, it is sufficiently accurate to write $S_r = S[1 + (2\gamma\Omega/kTr)]$ and this form of the equation is used in the subsequent analyses.

Equation (2.1) is readily extended to the case of non-spherical particle, provided they are close to an equilibrium shape. If the latter condition does not hold, the tendency to approach this shape will occur simultaneously with the coarsening process [17]. At the equilibrium shape, the right-hand side of the equation (2.1) becomes $(\Omega/kT) \partial(\sum A_i\gamma_i)/\partial V$, where V is the precipitate volume and A_i is the area of a face of the precipitate which has interfacial energy γ_i. Evaluation of this expression

6

is simplified by using the Wulff equation where x_i is the distance of the ith face from the centre of the precipitate [18] and equation (2 1) thus becomes

$$ln\left(\frac{S_x}{S}\right) = \frac{2\gamma_i\Omega}{kTx_i} \qquad (2.2)$$

Experimental evidence supporting the validity of equations (2.1) and (2.2) has been available for a long time [19] and has been obtained principally on salt solutions. The principal assumptions are that the solution is ideal and that the interfacial tension and particle density are independent of particle size. It has been demonstrated that interfacial tension may vary with radius of curvature but the effect is usually insignificant when particles are greater than 1 μ in radius [20]. Further, since the solutions to be considered are generally dilute, they can be considered ideal to a first approximation.

2.2.3 Estimation of Growth Rate

The driving force for particle growth is derived from the concentration gradients that exist in a system containing particles of different size. The solute concentration around any particle is known from equation (2.1) or (2.2). Immediately, however, we need to ask whether atoms can transfer sufficiently quickly across the interface between the particle and matrix for these concentration gradients to be maintained. When diffusion through the matrix is the rate controlling process, the particle growth is then said to be "diffusion-controlled". Conversely, when the most difficult step is for an atom to enter solution, the growth is then termed as "interface-controlled". It is next important to decide whether the diffusion gradients change significantly · with time or whether they may be regarded as almost time-independent. The latter is generally found to be a reasonable approximation and so Fick's First law is usually considered adequate to describe the diffusion gradients. An additional common assumption is that the solute diffusion coefficient is independent of solute concentration. Since, we usually consider dilute solutions, this assumption again would appear adequate.

The behaviour of any individual particle in the system under the condition that solute diffusion through the matrix is the rate limiting factor is first analysed. This particle may be growing or dissolving, depending on the solute concentration gradient near its surface, and the rate of change of particle radius is derived [21] from the equation

$$4\pi r^2\frac{dr}{dt} = 4\pi R^2 D\frac{dS}{dR} \qquad (2.3)$$

7

where dS/dR is the concentration gradient across an annulus at a distance R from the particle centre. Rewriting the equation after integration we obtain

$$\frac{dr}{dt} = -\frac{D\left(S_r - S_a\right)}{r}$$

(2.4)

where S_a is the average solute concentration a long distance from the particle and D is the diffusion coefficient. If the rate controlling step is the passage of material across the particle/matrix interface, then the rate of growth is given instead by the equation

$$\frac{dr}{dt} = -C\left(S_r - S_a\right)$$

(2 5)

where C is a constant and equation (2.5) replaces equation (2.4) when D is very much greater than the product Cr When D is of the same order of magnitude as Cr, allowance can be made [7] for the simultaneous importance of both time-dependent processes, such that equations (2.4) and (2.5) are the limiting cases, and the full equation then becomes

$$\frac{dr}{dt} = -C\,D\,\frac{\left(S_r - S_a\right)}{\left(C\,r + D\right)}$$

(2.6)

We now take into account further conditions which the system may approximately satisfy. When the particle solubility is small, the total number of atoms contained in the particles is constant, independent of particle-size distribution. This may be expressed as

$$\sum 4\,\pi\,r^2\,\frac{dr}{dt} = 0$$

(2.7)

Undue difficulties are not introduced if the particle solubility is not small and particles not widely spaced [22]. We can make a substitution for $\frac{dr}{dt}$ from equations (2.4), (2.5) or (2.6) into equation (2.7). Dealing first with the diffusion-controlled case, equation (2.4), we obtain

$$\sum -4\,\pi\,r_i\,D\left(S_{r_i} - S_a\right) = 0$$

(2.8)

Taking into account equation (2.1) we now make further substitution for S_{r_i} and we obtain the equation

$$\sum 4\,\pi\,r_i\,D\left[S_a - S\left(1 + \frac{2\,\gamma\,\Omega}{k\,T\,r_i}\right)\right] = 0$$
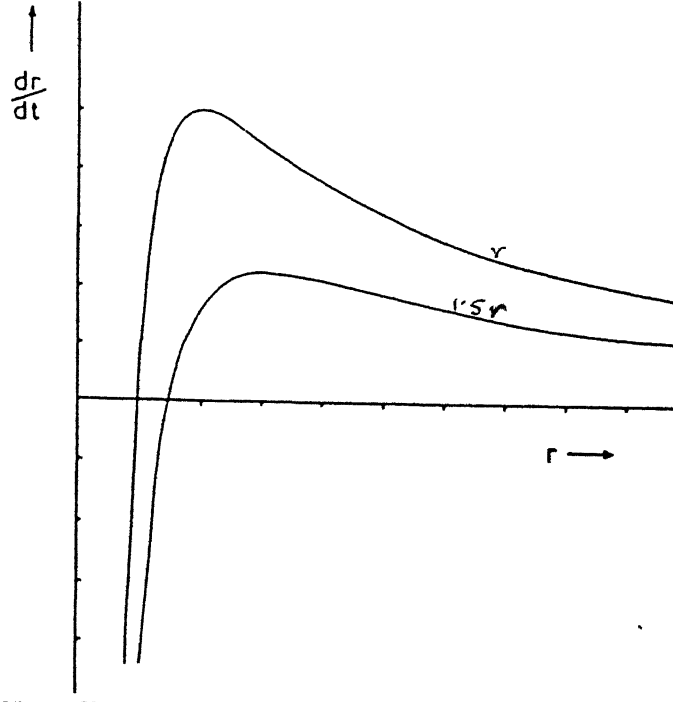
Figure 2.1. The variation of growth rate $\frac{dr}{dt}$ with particle radius r for diffusion-controlled growth.

On rearranging this equation, we can write

$$(S_a - S) \sum r_i = \sum \frac{2\gamma \Omega S}{kT}$$

$$= \frac{2n\gamma \Omega S}{kT}$$

where n is the total number of particles in the system at any instant and it is noted that the value of $\sum \frac{r_i}{n} = \bar{r}$, the arithmetic mean radius of the particles in the system. With this substitution again using equation (2.1), it follows that

$$S_a - S_r = \left(\frac{2\gamma \Omega S}{kT}\right) \left(\frac{1}{\bar{r}} - \frac{1}{r}\right) \tag{2.9}$$

Combining equations (2.9) and (2.4) we derive the increase in radius of any particle, which is thus given by the following equation

$$\frac{dr}{dt} = \left(\frac{2DS\gamma \Omega}{kTr}\right) \left(\frac{1}{\bar{r}} - \frac{1}{r}\right) \tag{2.10}$$

The variation of particle growth rate with radius is shown in Fig. 2.1. Particles of radius equal to the mean radius of the system are instantaneously neither growing nor dissolving. Particles of radius $< \bar{r}$ are dissolving at increasing rates with decreasing values of r. All particles of radius $> \bar{r}$ are growing but the graph shows a maximum value for the growth rate that corresponds to the particle which is twice the mean radius. Over a period of time the number of particles decreases discontinuously when

9

particles dissolve and disappear. It is a consequence of this that the system would ultimately tend to form one large particle. Long before reaching this state, however, the mean particle radius $\bar{r}$ increases as the number of particles decreases and thus the growth rate of the whole system slows down.

Fig. 2.1 has other interesting features. It is apparent that if all the particles were initially of the same radius there would be no growth in the system. Any slight deviation from this situation, however, leads to instability, since if any particles become even slightly greater than its neighbours that particle will continue to grow at their expense. Thus a particle-size distribution of limited range will become wider in its spread for increasing times. Even from the elementary analysis above, however, it is clear that the spread of particle sizes will be limited. This conclusion is reached because of the sharp maximum in Fig. 2.1 Although any particle of radius greater than twice the mean value continues to grow, it does so at a rate slower than that for particles which are somewhat smaller. It follows that particles which have a radius much more than twice the mean radius of the system cannot exist in the system. It is thus apparent that there must be some relatively sharp cut-off in the particle-size distribution curve. The above analysis indicates a cut-off at about twice the mean radius. More detailed analyses [6,7], reviewed later, confirm this general confinement of particle-size distribution though they indicate that particles which are more than 1.5 times the mean particle radius in size cannot continue to exist. The fuller analyses further indicate that the distribution reaches a pseudo-static form.

We next turn to the case where the growth kinetics is determined by interface control and begin by combining equations (2.5) and (2.7), from which it is deduced that

$$\sum -4\pi r_t^2 C (S_{r_t} - S_a) = 0 \qquad (2.11)$$

Using equation (2.1) and making further rearrangements

$$(S_a - S) \sum r_t^2 = \sum \frac{2\gamma \Omega S}{kT} r_i$$

So that $S_a - S_r = \frac{2\gamma \Omega S}{kT} \left[\left(\frac{\sum r_i}{\sum r_t^2} - \frac{1}{r} \right) \right]$ and by substituting from equation (2.5) we obtain

$$\frac{dr}{dt} = \frac{2 C \gamma \Omega S}{kT} \left[\left(\frac{\sum r_i}{\sum r_t^2} - \frac{1}{r} \right) \right] \qquad (2.12)$$

Equation (2.12) describe the growth rate of any particle when the kinetics depends on interface control and is analogous to equation (2.10), which describes the diffusion-controlled case.

The elementary analyses given above describe completely the physical parameters involved in a solution of the problem but they tell us nothing of the effect of spread of particle sizes or of the detailed change of particle distribution with time.

2.2.4 Particle Size Distribution

A particle-size distribution coefficient, f(r,t), can be defined that corresponds to the number of particles of a given radius r at time t. The total number of particles in the system at any instant is thus given by

$$z = \int_o^\infty f(r,t)\, dr \qquad (2.13)$$

When the particle-size distribution is initially narrow, z is constant. As the size distribution broadens, an increasing number of particles approach zero radius and disappear; thus z decreases with time. Using the following equation [7]

$$\frac{\partial f}{\partial t} = -\frac{\partial(fr)}{\partial r} \qquad (2.14)$$

We can deduce the rate of change of the total number of particles in the system is given by

$$\frac{dz}{dt} = -\frac{d}{dt}\left[\int_o^\infty f(r,t)\, dr\right] = \lim_{r \to 0}(fr) \qquad (2.15)$$

We can further describe the rate of decrease in average solubility as the particle size increases by the equation

$$\frac{dS}{dt} = \int_o^\infty \frac{4\pi r^2}{\Omega}\frac{dr}{dt}f(r,t)\, dr \qquad (2.16)$$

When particles have low solubility the rate of change of solubility must be small and as a first approximation equation (2.16) may be equated to zero. On making this approximation we can derive a value for the average concentration in the system in terms of the solute concentration in contact with a particle of infinite radius. Combining equations (2.16) and (2.6), which gives the growth for the general case of either interface- or diffusion-controlled growth, we obtain the rate of growth of any particle in the system.

$$\frac{dr}{dt} = \frac{-2\gamma\Omega S}{kTr}\frac{CD}{(Cr + D)}\left[1 - r\left(\frac{\int_o^\infty f(r,t)\, r\, dr\,/\,(Cr + D)}{\int_o^\infty f(r,t)\, r^2\, dr\,/\,(Cr + D)}\right)\right] \qquad (2.17)$$

Equation (2.17) gives results that are closely analogous to equation (2.10) when $Cr \gg D$ and to equation (2.12) when $Cr \ll D$.

11

The form of curve derived from equation (2 17) is not dissimilar from Fig 2.1. It leads, only in the diffusion-controlled case and not in the general case, to the simple prediction that the fastest growing particles is that which has twice the mean radius of the particles in the system. It does not indicate, however, that a narrow particle-size distribution will initially spread and that spreading will be restricted since very large particles in the system grow less rapidly than particles that are somewhat smaller. Equation (2 17) can be used to deduce the rate of change of the particle-size distribution with the time and to estimate the time required for the size distribution profile to reach a pseudo-static value. Further analysis derives from equations (2.14) and (2.17) in the form

$$\frac{\partial f(r,t)}{\partial t} = \frac{-2\gamma\Omega S}{kTr^*}\frac{\partial}{\partial r}\left[\frac{CD}{Cr+D}(r-r^*)\frac{f(r,t)}{r}\right] \qquad (2.18)$$

where r^* is the radius of a particle that is neither growing nor dissolving. To appreciate the implications of equation (2.18), we can either take an arbitrary initial particle-size distribution function or, more generally, manipulate the equation to show that a quasi-static distribution profile in terms of $\frac{r}{r^*}$ will ultimately be achieved which is independent of time.

Time-Dependence of Particle-Size Distribution

Wagner [7] showed how relatively simple expressions could be obtained from an initial particle-size distribution function assumed to take the form of a narrow Gaussian curve:

$$f(r,t=0) = S\,exp\left[\frac{-(r-\bar{r}_o)^2}{2\,\epsilon_o^2\,\bar{r}_o^2}\right] \qquad (2.19)$$

where $\bar{r}_o$ is the mean particle radius, $\epsilon\bar{r}_o$ is the standerd deviation and, since the distribution is narrow, $\epsilon_o \ll 1$. Substituting this value of f(r,t) in the growth equation (2.18) we obtain

$$\frac{d\epsilon}{dt} = \frac{2\gamma\Omega S}{\bar{r}_o^2\,kT}\frac{CD}{C\bar{r}_o+D}\,\epsilon$$

which has a solution for the value $\epsilon(t)$ at any time t given by

$$\epsilon(t) = \epsilon_o\,exp\left(\frac{t}{\tau}\right)$$

where τ is an effective time conatant for the rate of spread of the distribution and is expressed as

$$\tau = \frac{\bar{r}_o^2\,kT}{2\gamma\Omega S}\frac{C\bar{r}_o+D}{CD} \qquad (2.20)$$

The distribution is effectively stable unless the time allowed for growth is at least of the same order of magnitude as τ . For diffusion-controlled growth where $C\,\bar{r}_o \gg D$, we note that $\tau \propto \bar{r}_o^3$ and interface-controlled growth where $C\,\bar{r}_o \ll D$, then $\tau \propto \bar{r}_o^2$.

There is clearly a limit to the extent of spreading of the distribution in the above form when some particles begin to dissolve we first consider the case when diffusion transfer is rate controlling. From equation (2.10) we deduce that $\frac{dr}{dt} \propto r^{-2}$ for $r \ll \bar{r}$ and it follows that $f(r,t) \propto r^2$ for values of r near zero. Using this latter proportionality, it is convenient to write f(r,t) as the product of a time function g(t) and a particle-radius function $\rho^2\, h_1\,(\rho)$ where $\rho\, =\, r/r^*$, so that for $\rho \simeq 0$, $h_1\,(\rho)\, =\, 1$. Now in diffusion-controlled growth from equation (2.17), r^* equals the mean radius $\bar{r}$ since

$$r^*\ =\ \bar{r}\ =\ \frac{\int_o^\infty r\, f(r,t)\, dr}{\int_o^\infty f(r,t)\, dr}$$

Wagner [7] has shown how this equation can be satisfactorily solved and confirmed the finding of Lifshitz and Slyozov [6] that the solution corresponds to a quasi-stationary form of particle-size distribution, i.e. a distribution that retains the same profile when the abscissa is $= r/r^*\,(t)$. Thus $f(r,t)\ \propto\ \rho^2\, h_1(\rho)$ and it can be shown that

$$f(r,t)\ \propto\ \rho^3\, \left[\frac{3}{3+\rho}\right]^{7/3}\, \left[\frac{1.5}{1\,5-\rho}\right]^{11/3}\, exp\left[-\frac{\rho}{1.5-\rho}\right] \qquad (2.21)$$

for $\rho < 1.5$ and f(r,t) = 0 for $\rho > 1.5$. This implies a sharp cut off in the distribution such that no particles exist at long times that have a radius >1.5 times the mean radius of the distribution. The distribution has a maximum at $\rho = 1.135$ and the form of the distribution is shown in Fig. 2.2.

For times that are long compared with τ, an expression is derived for the approximate variation of mean particle radius with time

$$\bar{r}^3\ =\ \left[\frac{8\,D\,S\,\gamma\,\Omega\,t}{9\,k\,T}\right] \qquad (2.22)$$

for growth under diffusion-controlled conditions. We note that equation (2.22) is almost identical with the result of integrating equation (2.10) in the elementary theory and assumption that the mean radius is increasing at half the rate of that of the fastest growing particles.

The more detailed theory allows further predictions. Since the total volume fraction occupied by the dispersed precipitates is constant, the rate of change of the number of particles with the time dz/dt can be calculated. We arrive at an expression $z(t)\, =\, z_o/(1\, +\, \alpha\, t/\tau)$ where α is a constant $\simeq 4/9$. This equation is also similar to
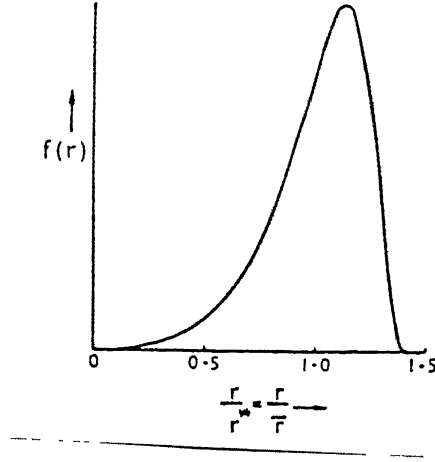
Figure 2.2: The form of particle-size distribution f(r) predicted after long period of time under conditions of diffusion-controlled growth.

the rate of change of the number of particles by colliding [23], but the latter process is unlikely to be of importance in solid matrices except perhaps when the precipitates are gas bubbles [24].

The case for interface-control can be treated in a way closely analogous to the above. The principal difference arises from the deduction from the equation (2.12) that now $dr/dt \propto 1/r$ for $r \ll \bar{r}$ and so in this case we consider the most useful particle-size distribution to take the form $\rho\, h_1(\rho)$. Since the particle radius r^* which is now neither growing nor dissolving is given from equation (2.17) by

$$r^* = \frac{\int_o^\infty r^2 f(r,t)\, dr}{\int_o^\infty r\, f(r,t)\, dr}$$

We again arrive at an equation for $h_2\,(\rho)$ similar to that derived for $h_1\,(\rho)$. Further requirements, however, which must be satisfied on the basis of equation (2.12) lead to the function $h_2\,(\rho)$ not being identical with $h_1\,(\rho)$ and a detailed analysis is again necessary. It is found that

$$\rho\, h_2(\rho) \ \propto \ f(r,t) \ \propto \ \rho \left[\frac{2}{2-\rho} \right]^5 exp \left[-\frac{3\rho}{2-\rho} \right] \tag{2.23}$$

for $\rho \le 2$ and f(r,t) = 0 for $\rho > 2$.

Again we have a cut-off in the particle-size distribution, which occurs at a particle radius equal to twice that of the particle which neither growing nor dissolving at the instant. The latter radius r^* can be shown [7] to be equal to $9\,\bar{r}/8$ and the shape of the curve is shown in Fig. 2.3.
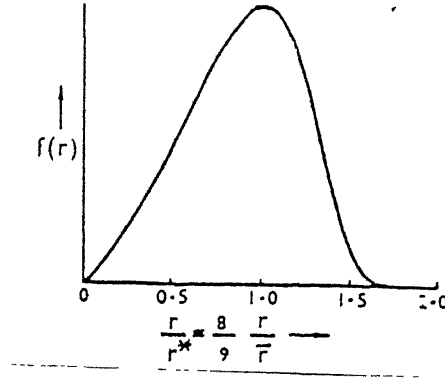
14

Figure 2.3: The form of particle-size distribution f(r) predicted after a long period of interface-controlled growth.

At long times $t \gg \tau$, the approximate relationship between mean particle radius and time for growth under interface-controlled conditions can be shown to be

$$\bar{r}^2 = \left[\frac{64\, C\, S\, \gamma\, \Omega\, t}{81\, k\, T}\right] \tag{2.24}$$

Thus we have equations that enable growth rates of systems to be assessed when the growth is predominantly by diffusion-control (equation (2.22)) or by interface-control (equation (2.24)). The expression relate growth rates to important physical parameters that can often be determined independently. Before turning to a comparison with experimental results in this field we consider the special case where diffusion processes do not take place isotropically through the matrix volume but are confined to grain boundaries.

2.2.5 Growth of Particles Situated on Grain Boundaries

Grain boundaries may play an important role in particle growth, since particles may tend to concentrate on grain boundaries by finding it easier to nucleate there. They may further pin the boundaries to restrict their movement because of the particle/grain boundary binding energy [25]. Especially at relatively low temperatures $(< \sim 0.6\ T_m)$ and when the mean particle size is small, the grain boundaries are the principal paths for transport between particles A treatment of this problem has been given for the diffusion-controlled case [9]. It is unlikely that the interface-controlled case would be important in practice, since the majority of solute atoms would be expected to leave the precipitates at areas away from the grain boundary.
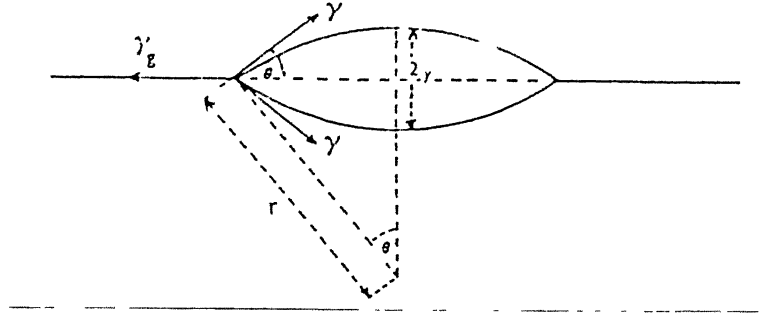
Figure 2.4: The simplest equilibrium shape of precipitate situated on a grain boundary consists of two spherical caps

It is first necessary to analyse the way in which the grain boundary influences the equilibrium particle size. Full analysis of this for particles with crystallographic faces, where equation (2.2) would normally apply, is complicated [26]. The analysis is much simpler for particles that would normally be spherical in shape. When situated on a grain boundary and with boundary tensions in equilibrium, such a particle takes a form bounded by two symmetrical spherical caps as in Fig. 2 4, the angle 2θ to their tangents at any point on the line of intersection being given by $\gamma_g = 2\gamma \cos\theta$, where γ_g is the grain boundary energy per unit area Developing a similar but somewhat more detailed argument than that behind equation (2.1), we find that

$$ln\left(\frac{S_r}{S}\right) = \frac{(2\gamma - \gamma_g)\,\Omega}{kTy}$$

where 2y is the thickness as defined in Fig. 2.4. We note that for $2\gamma < \gamma_g$ the equation does not hold, since the particle then spreads along the boundary and no longer has a discrete form. From the geometry of Fig. 2.4 we readily deduce that $(2\gamma - \gamma_g)/y = 2\gamma(1 - cos\theta)/y = 2\gamma/r$, where r is the radius of the spherical caps. Hence, we obtain a precisely analogous equation and there is no ambiguity in notation. Since r can be taken either as the radius of a cap for a grain-boundary particle or of an entire sphere when the particle is not on boundary.

The next step in the analysis is to determine the rate of change of particle volume in terms of the simplest geometrical parameters and this can be shown to be

$$\frac{dV}{dt} = \left[\frac{2}{3} - cos\theta + \frac{1}{3}cos^3\theta\right] 6\pi r^2 \frac{dr}{dt}$$

(2 25)

$$= \left[\frac{2}{3} - \left(\frac{\gamma_g}{2\gamma}\right) + \frac{1}{3}\left(\frac{\gamma_g}{2\gamma}\right)^3\right] 6\pi r^2 \frac{dr}{dt}$$

(2.26)

$$= 6\pi A r^2 \frac{dr}{dt}$$

(2.27)

where A is a constant defined as above for a given system.

Following the earlier treatment for diffusion-controlled particle growth, but now writing the steady-state equation for diffusion entirely confined to the of the boundary, we have

$$6\pi A r^2 \frac{dr}{dt} = 2\pi D_g x w \frac{dS}{dx}$$

(2.28)

where D_g is the solute diffusion coefficient in the grain boundary , w is the grain boundary width, and dS/dx the solute concentration gradient at a distance x from the particle centre. Integrating equation (2.28) we find

$$\frac{dr}{dt} = \frac{D_g w (S_{gL} - S_{gr})}{3 A r^2 ln(L/r)}$$

(2.29)

where S_{gr} is the solute concentration in the grain boundary adjacent to the particle surface and S_{gL} the concentration at a distance L away. Since the total volume of all particles is again constant $\sum r^2 dr/dt = 0$ and using this in conjunction with equation (2.29), then

$$\sum \frac{D_g w}{3 A ln(L/r_i)} \left[S_{gL} - S_g - \frac{2\gamma \Omega S_g}{kT r_i}\right]$$

(2.30)

where S_g is the solute concentration in the grain boundary near an infinitely large particle. Since usually L $\gg$ r, $ln(L/r_i)$ is approximately constant and can be written as B. Its value can be most simply estimated from the relation B $\simeq$ (1/2) ln(1/f), where f is the fractional area of grain boundary occupied by the particles. Continuing the analysis along the line developed earlier, the rate of growth of a particle of radius r_i is given by

$$\frac{dr_i}{dt} = \frac{2 D_g S_g w \gamma \Omega}{3 A B k T r_i^2} \left[\frac{\sum (1/r_i)}{n} - \frac{1}{r_i}\right]$$

(2.31)

17

Thus, any particle greater than the harmonic mean radius r_m at any instant is growing and particles smaller than this are dissolving. Particles of radius $r = 3r_m/2$ are growing at the faster rate and the maximum growth of particles over a period of time t, is for those whose radii remain close to this value throughout their growth. A full statistical analysis for the case of growth of particles on a grain boundary has not yet been developed, but one can observe by integrating of equation (2.31) that their growth will follow a law of the form

$$r_f^4 - r_o^4 = \frac{4\,D_g\,S_g\,\gamma\,\Omega\,w\,t}{3\,A\,B\,k\,T} \qquad (2.32)$$

from initial radius r_o to final radius r_f of the fastest growing particles. On average the particles will grow at a rate somewhat slower than predicted by equation (2.32) but generally particle growth expected to follow an equation of this form and the forth power of the average particle radius is thus expected to increase approximately linearly with time. This contrasts with the growth of precipitates by diffusion control where the diffusion flux takes place in three dimensions through the matrix. In the latter case the third power of the radius increases linearly with time.

This difference in the time-dependence of the change in average radius is not the only feature that in theory distinguishes the growth of precipitates on grain boundaries from the growth of precipitates within the grains. A major difference is that we are dealing with grain-boundary diffusion, which is characterised by an activation energy much less than that for the diffusion within the matrix. There is consequently a less-strong dependence on temperature for the growth of grain-boundary precipitates and for this reason their preferential growth likely to be predominant only at relatively low temperatures.

So far we have considered the growth of precipitates in the matrix and that of precipitates on the grain boundaries as being entirely separate processes. This is a convenient separation for theoretical analysis of the respective growth mechanisms, but it may well be less relevant to the modes of growth that can occur in practice. At some intermediate temperatures there is likely to be competition between particles on the grain boundaries and those within the grains. In particular, the shapes of the particles on the grain boundary (Fig. 2.4) are such that their effective size is governed by the radius of the spherical caps (equation (2.27)). Thus, a particle of given volume on a grain boundary has a larger driving force for growth when compared with a particle of the same volume within the matrix. Further, there may be change with time in the relative importance of grain boundary and matrix-growth processes. Initially, we may expect particles on grain boundaries to grow at a

18

relatively fast rate. Their growth rapidly decreases, however, as the average particle size increases (equation (2.31)) and at some stage grain boundary particles will tend to grow primarily at the expense of neighbouring particles situated within the matrix. This situation is likely to be a complicated one to analyse in detail and will depend on the particle sizes, concentration and grain size. It is conceivable that some systematic fluctuation in neighbouring particle sizes may be developed for particles within the grain. For example, those matrix particles adjacent to grain boundaries may dissolve in favour of the growth of the grain-boundary particles, but the particles in the matrix that are in the second row would initially tend to grow because of the depletion of the particles between them and the grain boundary Thus, there would be some tendency for alternate rows of particles to grow and dissolve on average, though the amplitude of these fluctuations would be expected to decrease rather rapidly with distance away from the grain boundary The importance of the processes outlined above has not yet been investigated experimentally. Possibly they are of no great importance because, at temperatures well below the melting point, the particle growth process is rather slow except when particles are very small and it may be that the average growth rate could generally be too slow to be of real significance except, perhaps, at relatively short times.

It is mentioned again that no case has been worked out for interface-controlled particle growth of grain-boundary particles. The reason for this is not difficult to find, since interface-controlled growth requires a given probability of atoms leaving any area of the particle surface. If atoms leave a particle not along the grain boundary, some diffusion through the lattice to the grain boundary is necessary. This implies that interface-controlled growth is unlikely to have a clearly defined relevance to the growth kinetics of particles on grain boundaries.

2.3 Experimental Studies of Particle Growth

The theoretical analyses previously outlined have not all received reliable experimental confirmation and at present firm support seems to have been provided only for the diffusion-controlled growth of particles within the matrix. The first measurements of growth rates followed the conditions specified in the earlier growth theories, namely, that the particles existed in a strain-free medium which was usually a liquid phase. Such experiments had the further advantage that diffusion in the liquid was rather faster and experiments could be done in somewhat shorter periods of time and for particle sizes that were relatively observed [21].

More recently, attention has been devoted to the coarsening of particles entirely in solid matrices and many such studies have been reported that cover both experimental and theoretical aspects [13, 14, 27-39]. Some measurements have been made of particles contained entirely within thin foils and examined by transmission electron microscopy [13,14]. Such measurements can then be made with considerable precision and it is especially interesting to know whether the theories are adequate to explain growth in the cases where one must also take into account the possible influence of strain fields induced by the particles and the further possibility of that interfacial energies vary with particle size. Recently it has also been shown feasible to obtain accurate quantitative measurements of particles too great to be accomodated entirely within thin foils yet too small to be observed by optical microscopy [40,41].

Increasing attention has placed on the method of plotting experimental results. It is only in the cases where the initial average radius of the particles is very small that it is appropriate to present results as a logarithmic plot of the variation of mean particle radius with time. In the more general case, where the mean initial radius of the particles of the system is not negligible, it is simpler to assume a law of particle growth and for example, plot the cube of the mean particle radius vs. time. Any departure from linearity in such a plot indicates that a wrong exponent of particle radius has been chosen or that an alternative relationship is required.

The first studies of particle coarsening in entirely solid system [27] were on a system involving cobalt particles dispersed in a copper matrix and used magnetic methods for average particle size measurement. The studies were aimed principally at the determination of a critical particle size for precipitation-hardening. The variation of mean particle radius with time, however, was also determined and showed quite clearly that r^3 was proportional to t. This work thus formed the basis of the first published account of experimental results supporting the theory of diffusion-controlled particle growth in a solid system. Of particular interest was the known coherency of small particles and the matrix in the system. The lattice misfit between copper and cobalt is relatively large (~2%), but despite the strain fields resulting from coherency the growth/time relationship appears unaffected. A re-assessment of the experimental results [14] has shown that there is a significant but not substantial change necessary in the value of some parameters of the growth equation (2.22) to obtain quantitative agreement between theory and experiment.

A considerable amount of further attention has recently been given to the influence on particle growth of strain due to coherency [42-44]. It has been convincingly argue that a coherent precipitate, because of its associated strain energy, must always

20

have a higher solubility than a noncoherent precipitate of the same phase. Although some alteration of the magnitudes of growth parameters is anticipated, serious modification to the general form of the growth analysis is not expected to be required [6].

The theory of particle coarsening by diffusion-control has also been applied to the case where particles have a markedly non-spherical shape. Studies of copper precipitates in an α-iron matrix [33] indicate that there is a large anisotropy in the particle/matrix interfacial free energy Despite this, the cube of the effective particle radius was again linearly proprotional to time. In this system, however, a number of complicating features may be envisaged in a quantitative analysis of the situation. In particular, since some coherency strains are likely, the particle shape would be modified from the true eqilibrium form determined purely by interfacial energy cinsidcrations. It is not surprising then that equation (2.22) does not predict growth rates precisely when the values of unmodified parameters are used in the theoretical calculation.

The most detailed information is on the Ni-Al system [13,14] where much work has been done on the coarsening of Ni_3Al (γ') particles. These studies have generally confirmed the relationship that the cube of the mean particle radius varies linearly with time and, in addition, since the size distribution of the particles has been measured, valuable statistical information has been obtained. The experimental results establish that there is a quasi-stationary particle-size distribution and a marked cut-off in the distribution curve The point of cut-off, however, tends to at a value rather higher than 1.5 times the mean particle radius but the form of curve is roughly similar to that predicted theoretically by Lifshitz and Slyozov [6] and Wagner [7]. On this point it is worth noting that, though the analysis of particle-size distributions is sound mathematically, the approximations implicit in the theory appear to result in some numerical discrepancies. From equation (2.10), and as illustrated in Fig. 2.1, the fastest growing particles are those of twice the mean radius of the system and it would thus be expected that there would be a cut-off in the particle-size distribution curve at a radius approximately equal to twice the mean radius. According to the statistical analysis of particle-size distributions from equation (2.21), which is also based on equation (2.10), particles that are greater than 1.5 times the mean radius do not exist.

In the nickel-aluminium system there is excellent agreement between experimental results and the predictions of equation (2.22) and no alterations to any parameters are required, despite evidence of clastic interaction between particles arising from the

21

difference between the elastic modulii of precipitate and matrix. These interaction effects are thus at most of only second-order importance in altering the kinetics of the growth process and either do not significantly change the solubility and solute diffusion coefficient or do so in a way such that their product remains essentially constant. One feature assisting the close agreement between theory and experiment in this system may be the isotropy of the particles which are in the form of cubes so that an effective particle radius can be readily defined. The agreement also persists when particles are close together and this may be accounted for by the dominating effect of solute concentration gradients near the particle surfaces [21].

Although the agreement between theory and experiment is generally less precise than in the case of the Ni-Al system, the usefulness of the theory is becoming evident in assessing the behaviour of an increasing number of other systems. An example is the growth of manganese precipitates in a magnesium-manganese alloy which have studied in some detail [38] and has involved observations of sufficient numbers of particles to obtain size-distribution curves. The cube of the mean particle radius was shown to vary linearly with time, suggesting diffusion-controlled growth, although the measured rate did not agree closely with the predictions of equation (2.22) when reasonable values were inserted for the parameters. It must be noted, however, that calculations from equation (2.22) often require a more precise knowledge than is available of the magnitudes of the parameters involved. In the particle-size distribution curves it was again noted that the cut-off point was at a particle radius > 1.5 times the mean radius of the system. The prediction of particles, existing at long times, of radius ~ twice the mean radius of the system which emerges as a consequence of equation (2.10) may be relevant in this connection, since it does not depend on subsequent approximations which are required in statistical development of the theory.

Some of the most interesting experimental cases involve precipitates that consists of two or more components, but a full analysis of the growth process in such instances is likely to be much more complicated [37]. The rate limiting cases must be considered and very often insufficient data are available to obtain quantitative information on the value of parameters which are required by theory. That unpredicted effects can be quite large is already clear from experimental work [45]. Particularly interesting cases concern those where one of the species may diffuse interstitially [36]. A rather special case involves the growth of iron-carbide particles in an iron matrix. It is clear in the later case that the coarsening rate of Fe_3C is too rapid for the diffusion of iron to be rate controlling but too slow for the process to depend solely on carbon diffusion when unmodified parameters are used. The reduced coarsening rate of Fe_3C

in alloys containing chromium has long been known and it is now well established that carbides with general formulae M_3C, M_7C_3 and $M_{23}C_6$ coarsen at rates very much less than Fe_3C [45]. It has been suggested that the coarsening of the series of carbides is related to the rate controlling step of chromium diffusion. A recent view is that, in general, growth is controlled by the slowest moving species but the diffusion coefficients and solubility may be affected by the stress gradients that surround the particles Further complications can arise when the matrix is unstable and recovery processes occur simultaneously with the particle coarsening.

The theory of particle coarsening limited by the rate of diffusion of solute from particle to particle is well sustained by experiments on a variety of systems. There does not yet appear to be firm experimental support for particle growth limited by interface control in entirely solid systems, although this condition may arise when particles with contaminated surfaces grow in a liquid phase through which solute diffusion is rapid [46].

Particle-size distribution curves have been found to assume a form which independent of time, in agreement with theory. There is some discrepancy, however, in the shape of the predicted curves and those measured experimentally. In particular, it appears from experimental results that particles which have a radius somewhat greater than 1 5 times the mean particle radius can continue to exist.

The theory of diffusion-controlled is not greatly modified when the precipitates produce strain in the matrix, though the parameters describing diffusion and solubility may be altered numerically.

The situation is more complicated when the particles consists of two or more components , both of which are different from the matrix. Growth may then be limited by the component that diffuses slowly but stress gradients surrounding the particles may be built up and may influnce growth.

At present there is no experimental evidence for the theory of particle growth for grain-boundary particles at temperatures well below the melting point, but the theory appears to be soundly based.

When the matrix is unstable, for example undergoing recrystallization or recovery, particle-coarsening rates are affected in a way that has not yet been analysed.

Chapter 3

Experimental Details

3.1 As Received Material

The composition of the steel, which is used in the present investigation, is given in the Table 3.1. The starting material was in the form of a strip having dimensions 10 cm X 1 cm X 0.5 cm.

3.2 Homogenization Treatment

To get homogeneous structure the initial material was austenitized at the temperature 900°C in a muffle furnace for 1 hour followed by furnace cooling. To prevent the oxidation and decarburization from the surface, the sample was kept in a box containing cast iron chips during the homogenizing treatment.

3.3 Tempering Treatment

After homogenizing treatment the initial material was cut into twenty two pieces having dimensions 0.5 cm X 0.5 cm X 0.5 cm. All of them were austenitised at 850°C

Elements	wt. %
C	0.65
Mn	1.5
Si	0.257
and the other elements in a very small amounts	

Table 3.1: Composition of the Eutectoid Steel used.

for 1 hour in a muffle furnace followed by water quenching. Among the twenty two samples two samples were kept separately to study the microstructure after quenching. Each of the twenty samples was given separate tempering heat treatment. Four different temperatures, 625, 650, 675, 700 and 725°C were choosen and at these temperatures four different holding times 2, 24 48 and 96 hours were selected.

3.4 Scanning Electron Microscopy

These samples were subjected to conventional metallographic polishing followed by etching using 2 % Nital (2 ml concentrated nitric acid and 98 ml ethyle alcohol). For quantitative metallography of the tempered microstructures scanning electron micrographs were taken using a **JEOL (JSM-840A)** scanning electron microscope at various magnifications. At least five micrographs of each sample at different magnifications were taken from different regions of the sample using secondary electron mode. Quantitative metallography was carried out with these micrographs.

3.5 Quantitative Metallography

The particle sizes were measured by line intercept method. The chord lengths were measured by putting a grid paper (2 mm square size) on the SEM micrographs of known magnifications. For each samples, at least five different micrographs taken from different regions at various magnifications were considered and then the average result was taken. Now to get the average radius of the cementite particles, this average chord length was multiplied by a multiplying factor of $\frac{4}{\pi}$ [47]. For each treatment on an average 300 particle sizes were measured.

Chapter 4

Results and Discussion

4.1 Microstructure

4.1.1 Annealed and Quenched Samples

Figure 4 1 (a) shows the microstructure of the annealed sample which reveals that it contains 100% pearlite. Figure 4.1 (b) shows the quenched structure which is fully martensitic.

4.1.2 Tempered Samples

It is well known that above $\sim 400°C$ complete cementite precipitation from martensite occurs in a very short period and only coarsening of cementite particles occurs on prolonged temperating. Figure 4.2 to 4.6 shows the representative SEM micrographs of the different samples tempered at different temperatures and times. From these micrographs it is clear that the cementite particles are approximately spherical and distributed throughout the matrix.

4.2 Quantitative Metallography

Table 4.1 gives the average particle size and Table 4.2 to 4.6 gives the particle size distribution data of cementite particle at different tempering temperature and time. The average particle size is plotted against cube root of time in Figure 4.7. It is seen that the average particle size varies linearly with cube root of time. This conforms to Lifshitz-Slyozov-Wagner theory of particle coarsening by volume diffusion control i.e.

$$\bar{r}^3 \quad = \quad k\,t \qquad (4.1)$$

or

$$\bar{r} = k' t^{1/3} \qquad (4\ 2)$$

where, $\bar{r}$ is average particle size, t is coarsening time and k is rate constant the rate constant k is given by·

$$k = k_o\ exp(-Q/RT) \qquad (4\ 3)$$

where, k_o is constant, R is gas constant, T is temperature in degree Kelvin and Q is the activation energy for the rate controlling step. The rate constant k obtained from the plots in Figure 4.7 is tabulated in Table 4.7. In Figure 4.8 the logarithm of the rate constant k, is plotted against reciprocal of absolute temperature. The slope of the curve in Figure 4.8 gives the activation energy of cementite coarsening as 82 65 kJ/mol. This activation energy value compares very well with the value of 83 kJ/mol given by Mukherjee et al. [45]. The activation energy for carbon diffusion in ferrite is 83.5 kJ/mol. [48]. Hence it can be concluded cementite coarsening is controlled by volume diffusion of carbon in ferrite.

According to the LSW theory of particle coarsening by volume diffusion control, the particle size distribution during coarsening attains a pseudo-steady state condition. This pseudo-steady state distribution is given as:

$$f(r,t) \propto \rho^3 \left[\frac{3}{3 + \rho}\right]^{7/3} \left[\frac{1\ 5}{1.5 - \rho}\right]^{11/3} exp\left[-\frac{\rho}{1.5 - \rho}\right] \qquad (4.4)$$

where, f(r,t) is the particle size distribution coefficient, ρ is radius ratio i.e, $r/\bar{r}$. For $\rho < 1.5$ and f(r,t) = 0 for $\rho > 1.5$. This implies a sharp cut off in the distribution such that no particles exist at long times that have a radius >1.5 times the mean radius of the distribution. The distribution has a maximum at $\rho = 1.135$. A closer look at the data in Tables 4.2 to 4.6 shows that a pseudo-steady state distribution exists during the coarsening process at different temperature and time. The relative particle size distribution data for some representative treatments, are plotted in Figure 4.9 to 4.12. Also plotted in these figures is the relative particle size distribution calculate from equation (4.4). The experimental relative size distribution compares very well with the theoretically expected size distribution. Negligible number of particles with sizes $> 1.5\bar{r}$ is found in all the treatment as predicted by the LSW theory.
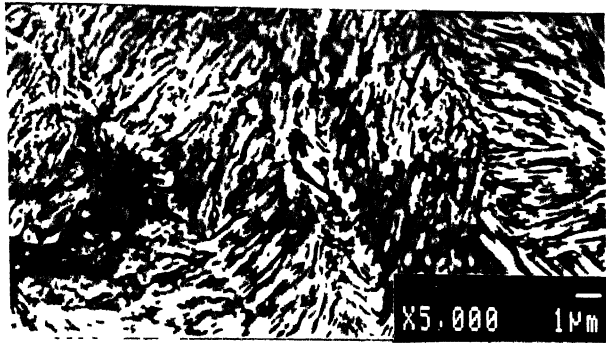
a
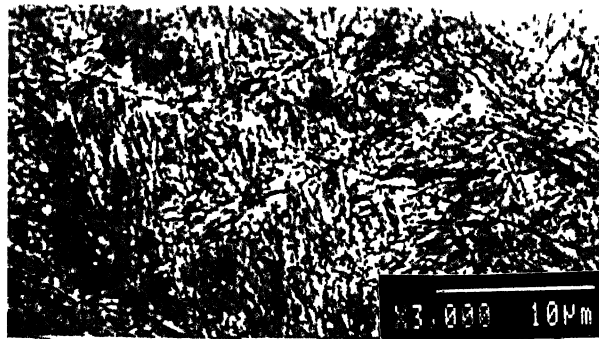
b

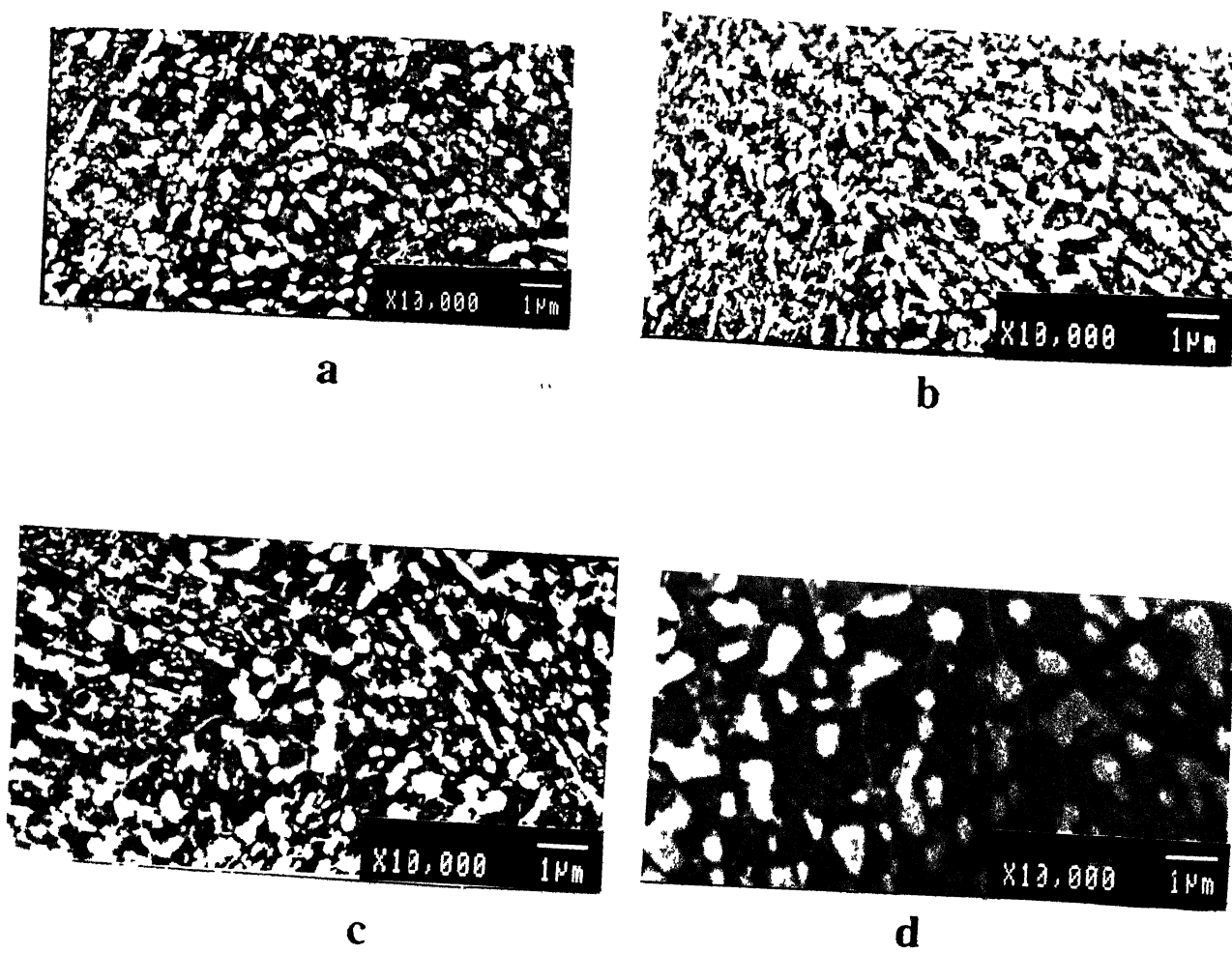Figure 4.1: SEM micrographs of the a) as received and b) quenched sample.

Figure 4.2: SEM micrographs of the Sample Tempered at 625°C for a) 2 hours, b) 24 hours, c) 48 hours and d) 96 hours.
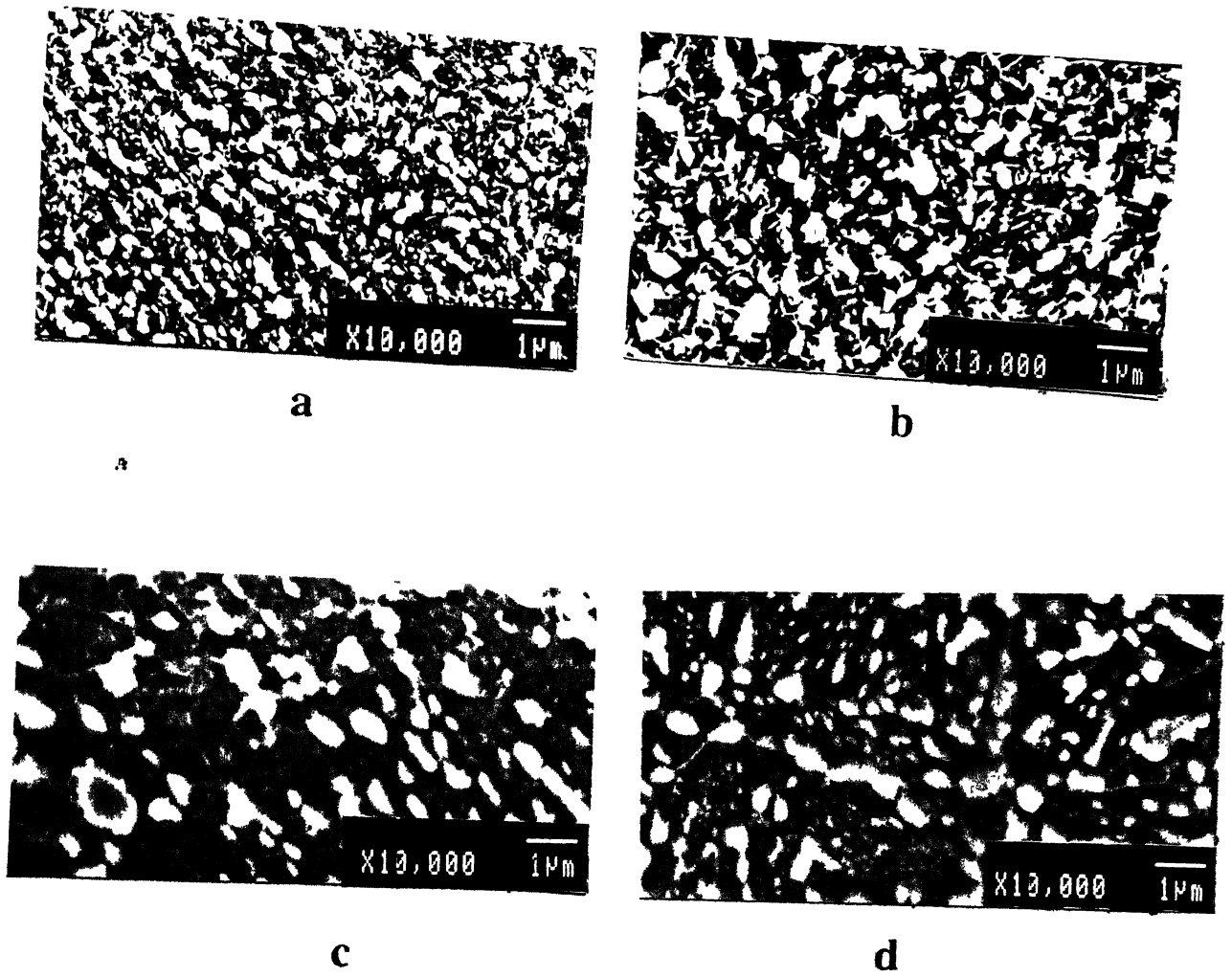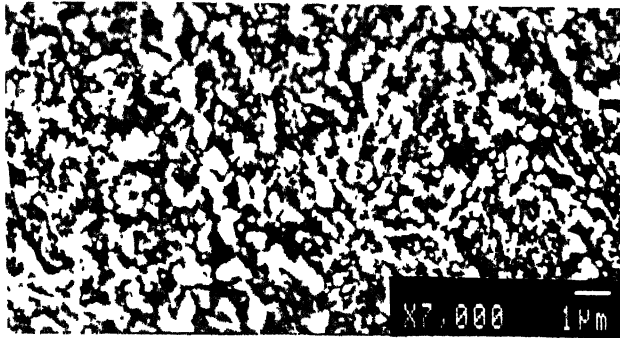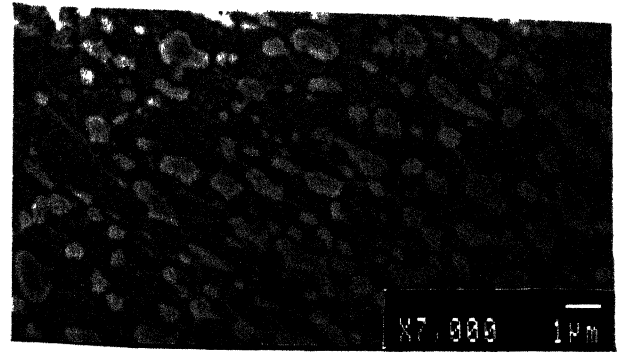
Figure 4.3: SEM micrographs of the Sample Tempered at 650°C for a) 2 hours, b) 24 hours, c) 48 hours and d) 96 hours.

Figure 4.4: SEM micrographs of the Sample Tempered at 675°C for a) 2 hours, b) 24 hours, c) 48 hours and d) 96 hours.
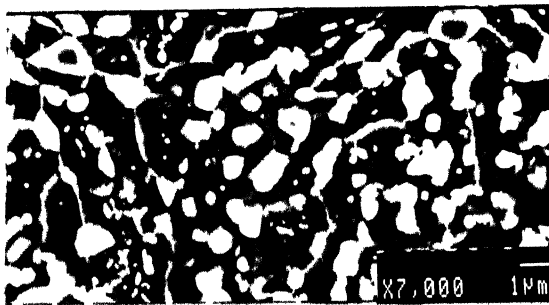
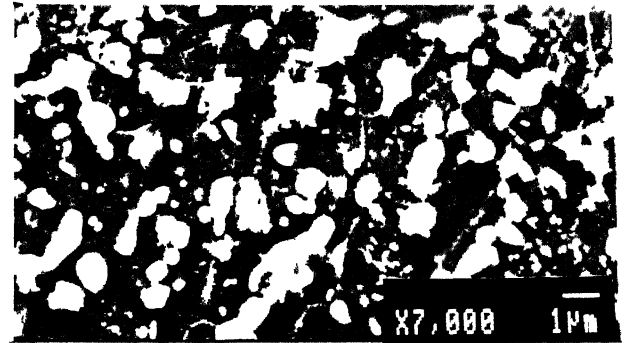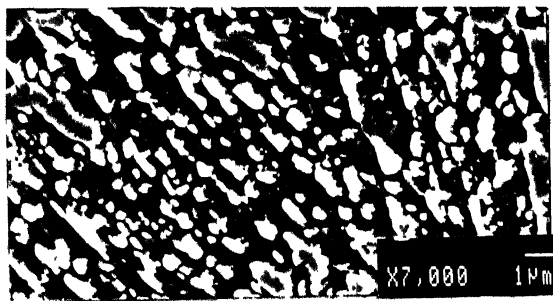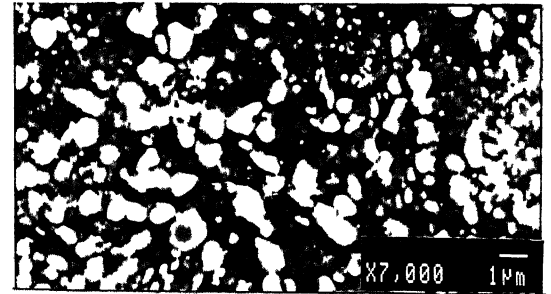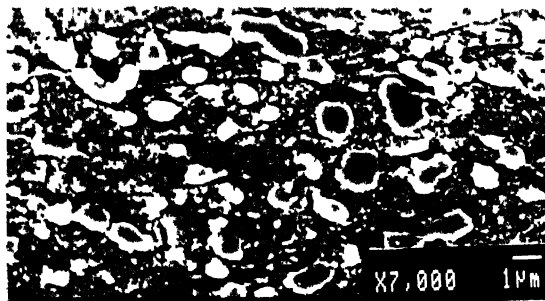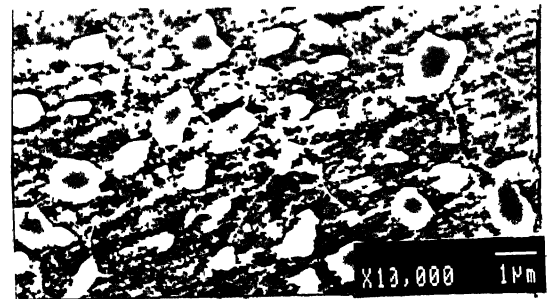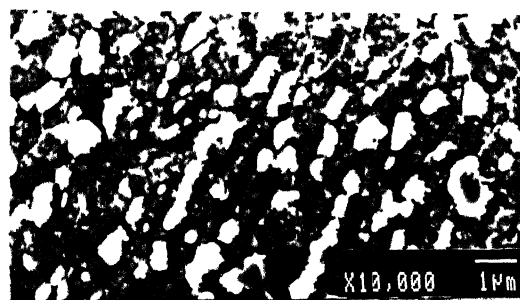Figure 4.5: SEM micrographs of the Sample Tempered at 700°C for a) 2 hours, b) 24 hours, c) 48 hours and d) 96 hours.

Figure 4.6: SEM micrographs of the Sample Tempered at 725°C for a) 2 hours, b) 24 hours, c) 48 hours and d) 96 hours.

Temp	Time in Hours			
(°C)	2	24	48	96
625	40	96	122	152
650	47	105	136	174
675	53	116	145	185
700	55	127	158	197
725	61	137	178	220

Table 4.1: Average Particle Size (nm) as a Function of Tempering Temperature and Time.

$\frac{r}{\bar{r}}$	Number of Particles			
	2 hrs.	24 hrs.	48 hrs.	96 hrs.
0.0 - 0.05	0	0	0	0
0.05 - 0.15	1	1	1	1
0.15 - 0.25	2	2	2	2
0.25 - 0.35	4	3	4	4
0.35 - 0.45	7	8	6	7
0.45 - 0.55	11	11	12	13
0.55 - 0.65	16	15	20	21
0.65 - 0.75	25	27	30	34
0.75 - 0.85	35	36	41	45
0.85 - 0.95	45	48	53	58
0.95 - 1.05	55	60	62	69
1.05 - 1.15	42	41	47	56
1.15 - 1.25	25	26	28	35
1.25 - 1.35	15	13	17	15
1.35 - 1.45	10	6	4	3
1.45 - 1.50	4	2	2	1

Table 4.2: Particle Size Distribution Data for the Sample Tempered at 625°C.

$\frac{r}{\bar{r}}$	Number of Particles			
	2 hrs.	24 hrs	48 hrs.	96 hrs
0.0 - 0.05	0	0	0	0
0 05 - 0 15	1	1	1	1
0 15 - 0.25	2	2	2	2
0.25 - 0 35	4	4	4	4
0.35 - 0.45	7	7	7	6
0.45 - 0.55	11	13	12	12
0.55 - 0.65	16	18	17	17
0.65 - 0.75	25	26	25	23
0.75 - 0.85	35	34	35	36
0.85 - 0.95	45	42	43	42
0.95 - 1.05	49	51	53	52
1.05 - 1.15	56	56	57	58
1.15 - 1.25	35	34	34	32
1.25 - 1.35	15	15	13	14
1.35 - 1.45	3	4	4	4
1.45 - 1.50	1	1	2	2

Table 4.3: Particle Size Distribution Data for the Sample Tempered at 650°C.

$\frac{r}{\bar{r}}$	Number of Particles			
	2 hrs.	24 hrs.	48 hrs.	96 hrs.
0.0 - 0.05	0	0	0	0
0.05 - 0.15	1	1	1	1
0.15 - 0.25	2	2	2	2
0.25 - 0.35	4	5	5	5
0.35 - 0.45	7	9	7	8
0.45 - 0.55	11	12	11	13
0.55 - 0.65	18	20	19	20
0.65 - 0.75	25	24	27	27
0.75 - 0.85	37	37	39	40
0.85 - 0.95	45	46	48	50
0.95 - 1.05	59	58	64	65
1.05 - 1.15	66	64	50	42
1.15 - 1.25	45	34	29	25
1.25 - 1.35	16	20	18	15
1.35 - 1.45	2	4	9	5
1.45 - 1.50	1	2	1	1

Table 4.4: Particle Size Distribution Data for the Sample Tempered at 675°C.

$\frac{r}{\bar{r}}$	Number of Particles			
	2 hrs.	24 hrs.	48 hrs	96 hrs.
0.0 - 0.05	0	0	0	0
0.05 - 0.15	1	1	1	1
0.15 - 0.25	2	2	2	2
0.25 - 0.35	5	5	5	4
0.35 - 0.45	8	6	7	7
0.45 - 0.55	13	11	12	11
0.55 - 0.65	20	17	18	16
0.65 - 0.75	27	27	26	25
0.75 - 0.85	40	39	36	35
0.85 - 0.95	50	46	47	·45
0.95 - 1.05	65	58	62	49
1.05 - 1.15	42	36	40	56
1.15 - 1.25	25	18	27	35
1.25 - 1.35	15	13	16	15
1.35 - 1.45	5	4	6	3
1.45 - 1.50	1	1	2	1

Table 4.5: Particle Size Distribution Data for the Sample Tempered at 700°C.

$\frac{r}{\bar{r}}$	Number of Particles			
	2 hrs.	24 hrs.	48 hrs.	96 hrs.
0.0 - 0.05	0	0	0	0
0.05 - 0.15	1	1	1	1
0.15 - 0.25	2	2	2	2
0.25 - 0.35	4	4	4	4
0.35 - 0.45	7	6	8	7
0.45 - 0.55	13	11	12	11
0.55 - 0.65	21	17	20	18
0.65 - 0.75	34	31	27	25
0.75 - 0.85	45	40	41	37
0.85 - 0.95	58	56	51	45
0.95 - 1.05	69	68	60	59
1.05 - 1.15	56	51	68	66
1.15 - 1.25	35	32	40	45
1.25 - 1.35	15	14	17	16
1.35 - 1.45	3	2	10	2
1.45 - 1.50	1	1	1	1

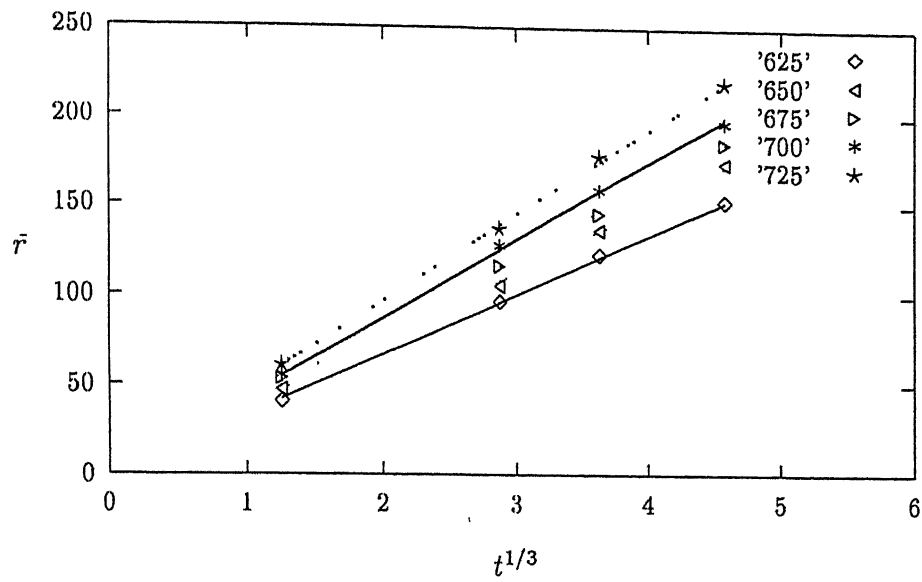Table 4.6: Particle Size Distribution Data for the Sample Tempered at 725°C.

Figure 4 7: Average Cementite Particle Size vs Cube Root of Time as a Function of Different Tempering Temperatures.

k (nm^3/hr)	$\frac{1}{T} \times 10^{-3}$ (K^{-1})
36570.608	1.114
52739.520	1.083
65569.927	1 005
81845.640	1.028
110884.09	1.002

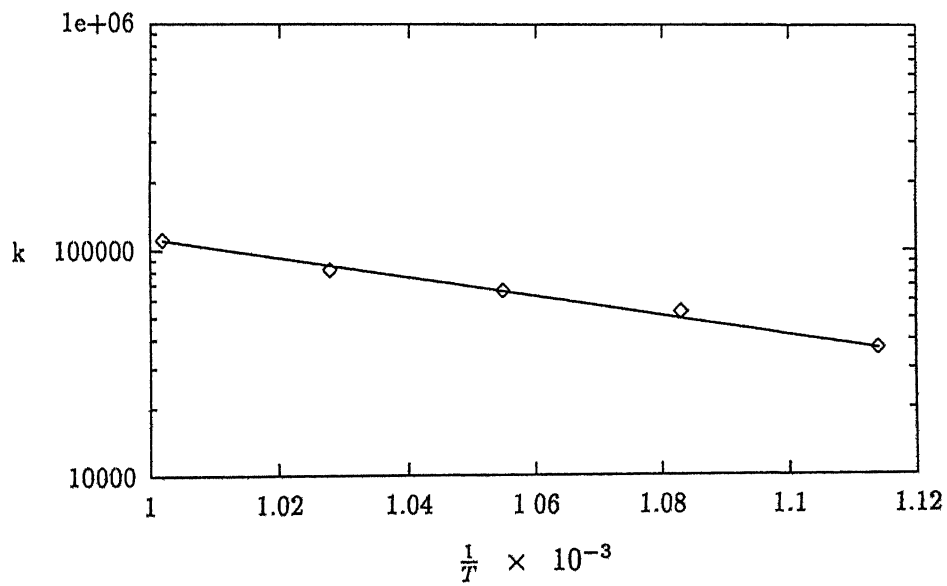Table 4.7: Rate Constants from Figure 4.7 and Corresponding Reciprocal Absolute Temperatures.

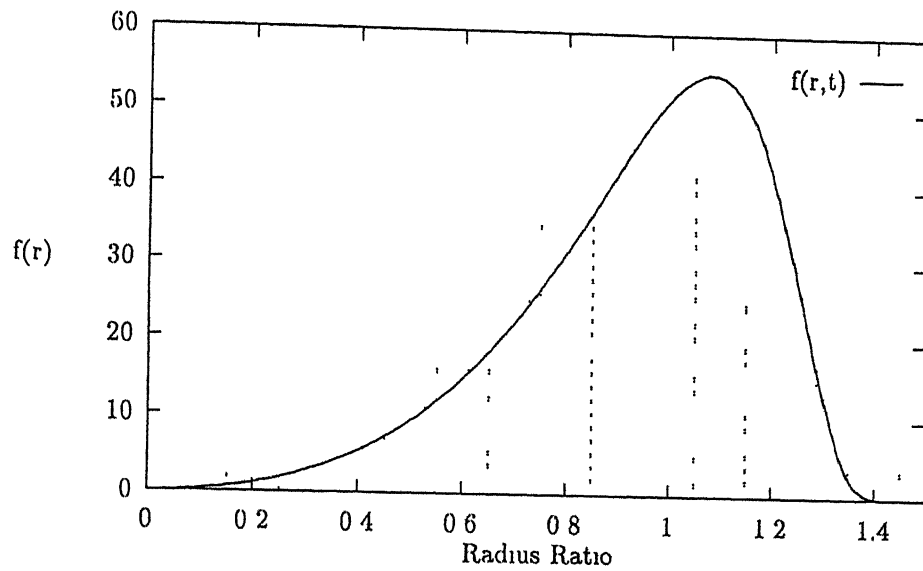Figure 4.8: Logarithm of the Rate Constants vs. Reciprocal of Absolute Temperatures.

Figure 4 9: Particle-size Distribution Curve for the Sample Tempered at 625° for 2 hours.
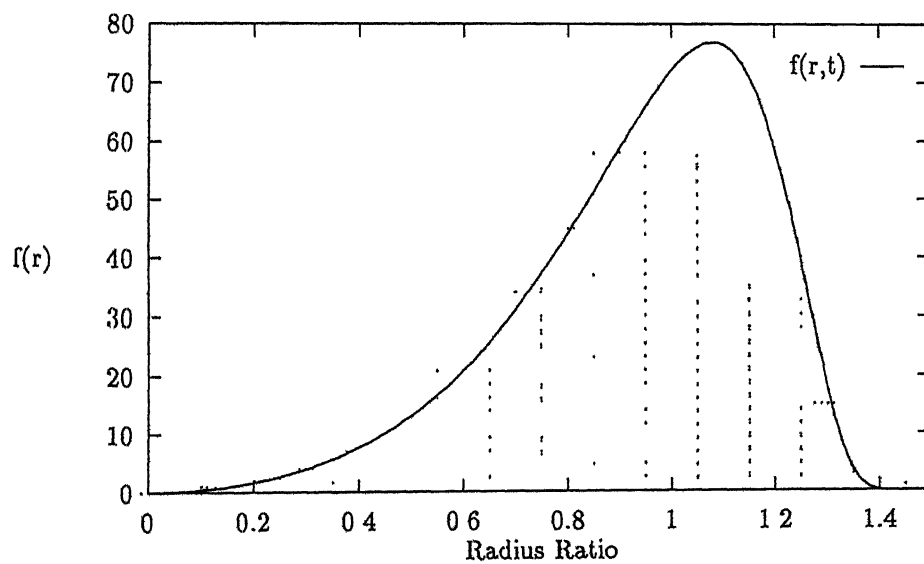

Figure 4.10: Particle-size Distribution Curve for the Sample Tempered at 625° for 96 hours.
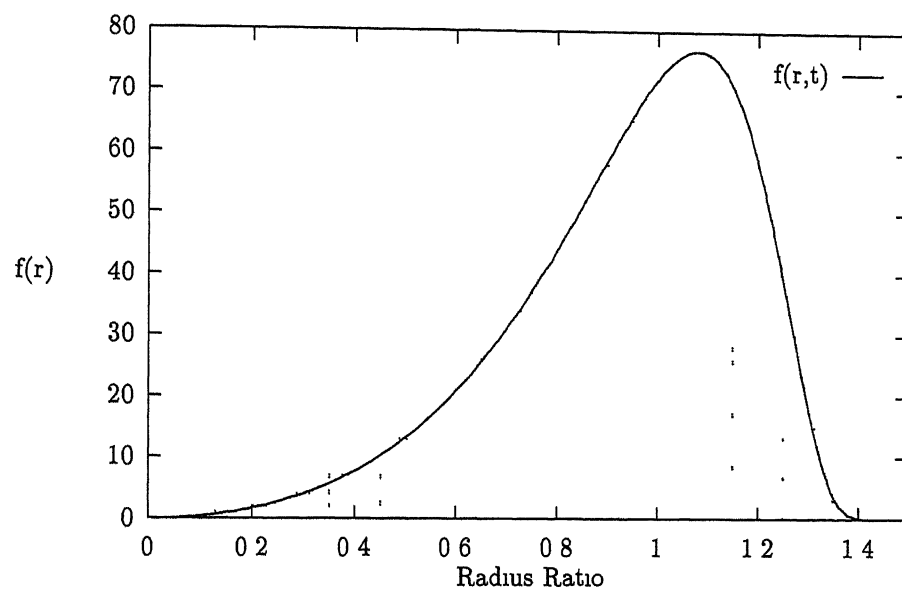
Figure 4.11: Particle-size Distribution Curve for the Sample Tempered at 725° for 2 hours.
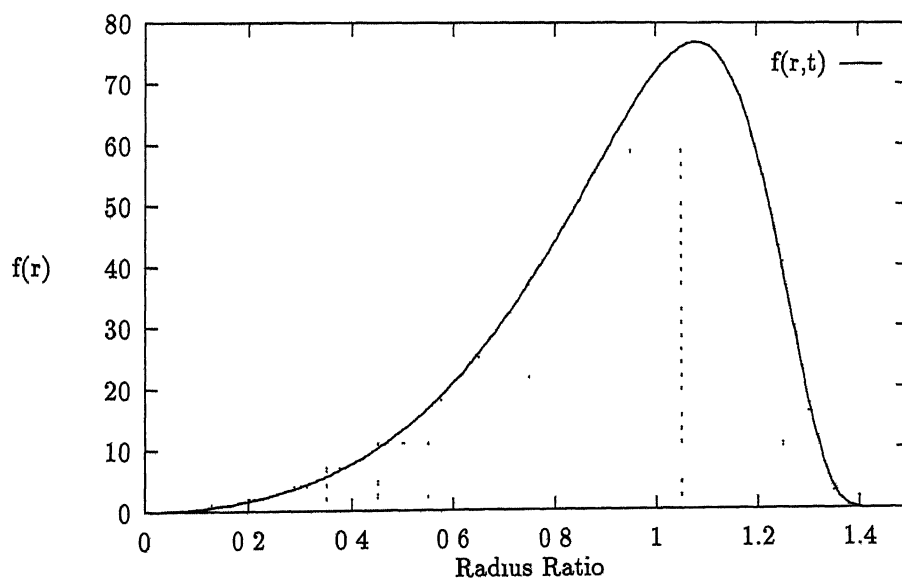

Figure 4.12: Particle-size Distribution Curve for the Sample Tempered at 725° for 96 hours.

Chapter 5

Conclusions

From the present investigation of the kinetics of cementite coarsening in quenched and tempered eutectiod steel, the following conclusions are arrived at:

1. The cementite coarsening occurs by volume diffusion control according to the LSW theory, i.e , the average particle size varies as cube root of time.

2. The activation energy for cementite coarsening process is obtained as 82.65 kJ/mol. This compared well with the activation energy for carbon volume diffusion (83.5 kJ/mol) in ferrite.

3. Size distribution of cementite particles maintains a pseudo steady state condition during coarsening process as expected from the LSW theory.

References

1. Raymond A. Higgins in Engineering Metallurgy, Part-I: Applied Physical Metallurgy, ELBS ed., 1993.

2. George E. Dieter in Mechanical Metallurgy, 3rd Ed., McGraw-Hill Books Co., New York, 1987.

3. F. Borik and R. D. Chapman, *Trans. Am. Soc. Met.*, vol-53, 1961.

4. M. F. Garwood, H. H Zurburg and M A. Erichson in Interpretation of Tests and Correlation with Service, ASM, Metals Park, Ohio 1951

5. D. A. Porter and K. E. Easterling in Phase Transformations in Metals and Alloys, Van Nostrand Reinhold Co., New York, 1981.

6. I. M. Lifshitz and V. V. Slyozov, *J Physics Chem. Solids*, vol-19, 1961, p-35.

7. C. Wagner, *Z. Elektrochem.*, vol-65, 1961, p-581.

8. V. V. Slyozov and I. M. Lifshitz, *Soviet Physics-Solid State*, vol-1, 1960, p-1285.

9. M. V. Speight, *Acta Met.*, vol-16, 1968, p-133.

10. H. O. K. Kirchner, *Met. Trans.*, vol-2A, 1971, p-2261.

11. G. Kurdjumov and G. Sachs, *Z. Physik*, vol-64, 1930, p-325.

12. A. J. Ardell and R. B. Nicholson, *Acta Met.*, vol-14, 1966, p-1295.

13. A. J. Ardell and R. B. Nicholson, *J. Physics Chem. Solids*, vol-27, 1966, p-1793.

14. A. J. Ardell, *Acta Met.*, vol-20, 1972, p-601.

15. Robert E. Reed-Hill in Physical Metallurgy Principles, 2nd Ed , Affiliated East-West Press Pvt. Ltd., New Delhi, 1973.

16. H. Freundlich, "Kapillarchemie", Leipzig (Akad. Verlagsgesellschaft m.b.h), 1922.

17. P. J. Barton and G. W. Greenwood, *J. Inst. Metals*, vol-86, 1957-8, p-504.

18. G. Wulff, *Z. Krist.*, vol-34. 1901, p-495.

19. W. Ostwald, *Z. Physikal Chem.*, vol-34, 1900, p-243.

20 W. A. Patrick and N. F. Eberman, *J. Phys. Chem.*, vol-29, 1925, p-227.

21. G. W. Greenwood, *Acta Met.*, vol-4, 1956, p-243.

22. R. Asimov, *Acta Met.*, vol-11, 1963, p-72.

23. M. von Smoluchowski, *Z. Physik*, vol-17, 1916, p-557.

24. G. W. Greenwood and M V. Speight, *J. Nuclear Mat*, vol-10, 1963, p-140.

25. D. Mclean in Grain Boundaries in Metals, Oxford (Clarendon Press): 1957

26. R. S. Nelson, D. J. Mazey and R. S Barnes, *Phil. Mag.*, vol-11, 1965, p-91.

27. J. D. Livingstone, *Trans. Met. Soc. A. I M E.*, vol-215, 1959, p-566.

28. A. Dromsky, F. V. Lenel and G. S. Ansel, *ibid.*, vol-224, 1962, p-236.

29. O. Bonnyh, H. Modin and S. Modin, *Jernkontorets Ann*, vol-146, 1962, p-774.

30. R. A. Oriani, *Acta Met.*, vol-12, 1964, p-1399.

31. N. Komatsu and N. J. Grant, *Trans. Met. Soc. A. I. M. E.*, vol-230, 1964, p-1090.

32. R. W. Heckel, *ibid.*, vol-233, 1965, p-1994

33. G. R. Speich and R. A. Oriani, *ibid.*, p-623.

34. R. W .Heckel and R. C. De Gregorio, *ibid.*, p-2001

35. R. W. Heckel and J. Buchwald, *ibid.*, p-1798.

36. J. E. Harris, J. A. Whiteman and A. G. Quarrell, *ibid.*, p-168.

37. G. B. Gibbs, *ibid.*, p-1969.

38. A. F. Smith, *Acta Met.*, vol-15, 1967, p-1867.

39. J. S. Hirshhorn, *Metal Sci. J.*, vol-1, 1967, p-91.

40. C. M. Sellars and A. F. Smith, *J. Mat. Sci.*, vol-2 ,1967, p-221

41. T. Mukherjee, W. E. Stumpf, C. M. Sellars, *ibid.*, vol-3, 1968, p-127.

42. J. W. Chan, *Acta Met.*, vol-10, 1962, p-907.

43. J. W. Chan, *ibid.*, vol-14, 1966, p-83

44. R. A. Oriani, *ibid.*, p-84.

45. T. Mukherjee, W. E. Stumpf, C. M Sellars, and W. J. McG. Tegart, *J. Iron Steel Inst.*, vol-207, 1969, p-621.

46. S. Sarian and H. W. Weart, *J. Appl. Physics*, vol-37, 1966, p-1675.

47. E R. Weibel in Stereological Methods, Part II, Academic Press, 1979.

48. V. Raghavan in Materials Science and Engineering, Prentice Hall India, New Delhi, 1991.

Date Slip

This book is to be returned on the
date last stamped.

MME-1996 - M-GHO-KIN